

ornl

ORNL/M--5050

C/Y-1293-0211

**OAK RIDGE
NATIONAL
LABORATORY**

LOCKHEED MARTIN



**CRADA FINAL REPORT
for
CRADA Number C/Y-1293-0211**

GELCASTING OF SOFT FERRITE PARTS

O. O. Omatete
G. L. Van Dillen, Jr.

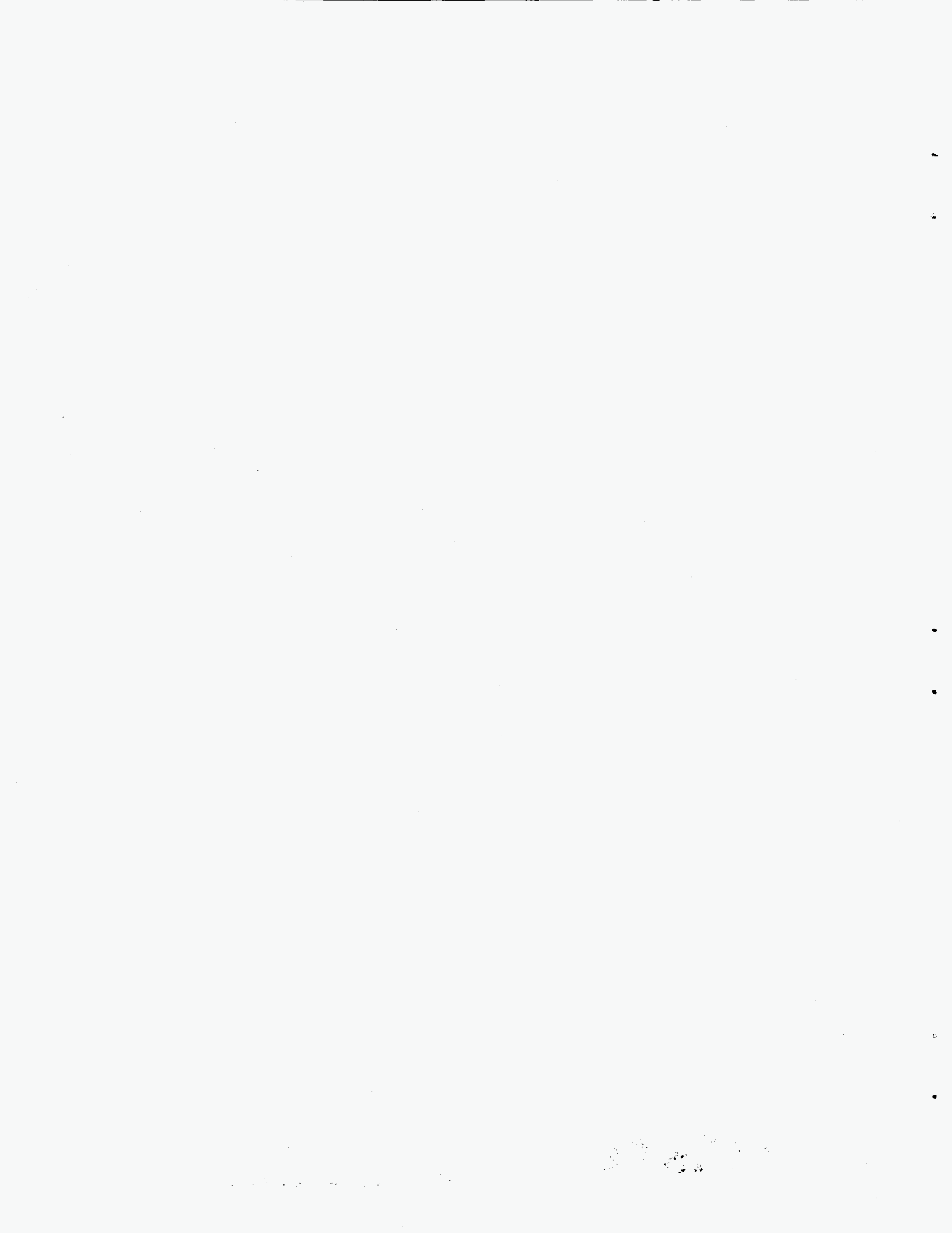
Prepared by the Oak Ridge National Laboratory
Oak Ridge, Tennessee 37831-6285
managed by
LOCKHEED MARTIN ENERGY RESEARCH INC.
for the
U. S. DEPARTMENT OF ENERGY
under contract DE-AC05-96OR22464

Approved for
Public release;
distribution is
unlimited.

MANAGED AND OPERATED BY
LOCKHEED MARTIN ENERGY RESEARCH CORPORATION
FOR THE UNITED STATES
DEPARTMENT OF ENERGY

ORNL-27 (3-96)

MASTER



C/Y-1293-0211

**CRADA FINAL REPORT
for
CRADA Number C/Y-1293-0211**

GELCASTING OF SOFT FERRITE PARTS

**O. O. Omatete
Oak Ridge National Laboratory**

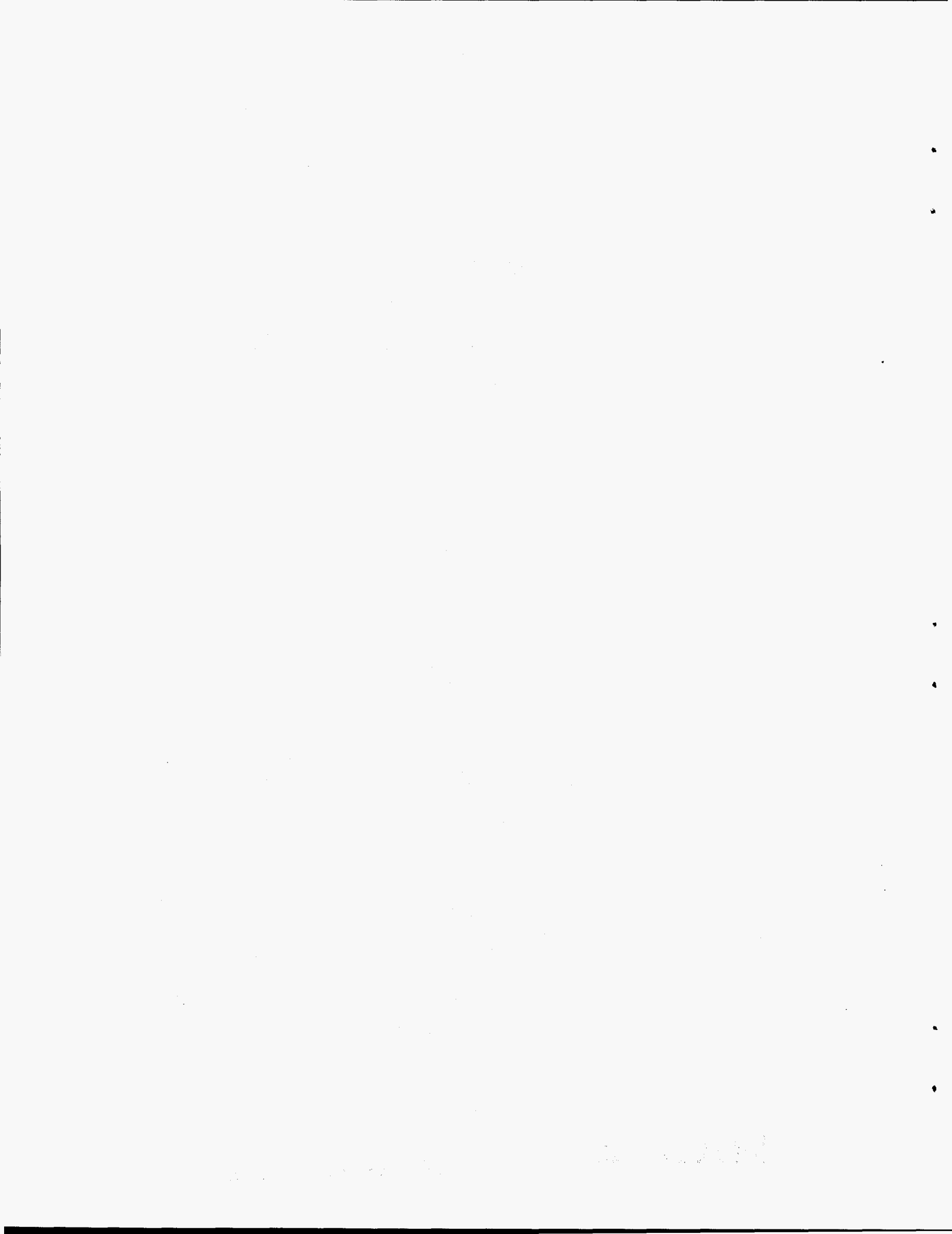
**G. L. Van Dillen, Jr.
Ceramic Magnetics, Inc.**

Date Published: March 1996

Prepared by the Oak Ridge National Laboratory
Oak Ridge, Tennessee 37831-6285
managed by
LOCKHEED MARTIN ENERGY RESEARCH INC.
for the
U. S. DEPARTMENT OF ENERGY
under contract DE-AC05-96OR22464

MASTER

DISTRIBUTION OF THIS DOCUMENT IS UNLIMITED HH



Final Report on the Cooperative Research and Development Agreement (CRADA)
No. Y-1293 - 0211 between Ceramic Magnetics, Inc., and Martin Marietta Energy
Systems (MMES)

Ogbemi O. Omatete, Principal Investigator, Martin Marietta Energy Systems
G. Lawrence Van Dillen, Jr., Principal Investigator, Ceramic Magnetics, Inc.

GELCASTING OF SOFT FERRITE PARTS

ABSTRACT

Soft ferrite parts utilized in areas such as high-energy physics have been successfully gelcast from powders supplied by the industrial partner. To achieve this, several modifications were necessary. First, the as-received ferrite powder was heated to 300, 500 or 800°C. X-ray analysis showed no changes in the crystal structure of the heat-treated powder even at 800°C, and particle size distribution and surface area analyses indicated that powders heat treated at 300 and 500°C had mean size and surface area similar to those of the as-received powder. Second, to prevent the parts from shattering during the combined binder burn-off and sintering cycle, the solids loading of the gelcasting slurry was adjusted from 42 vol % to at least 50 vol % and the sintering schedule was modified slightly. These modifications resulted in the production of fired gelcast soft ferrite parts (50 mm x 13 mm pucks, ~ 125 mm OD x 100 mm ID x 25 mm rings) which sintered to ~98% of the theoretical density. The partner was satisfied with the parts it received and has discussed pursuing follow-up activities in order to gelcast more complex shapes and large toroids.

INTRODUCTION

The primary objective of this CRADA was to apply gelcasting, a ceramic forming process developed at the Oak Ridge National Laboratory, to the fabrication of soft ferrite parts from the powders supplied by the partner. This primary objective was accomplished successfully. A second objective was to gelcast complex-shaped and large-toroidal parts. This second objective was not completed before the CRADA expired.

Benefits to DOE Programs The Department of Energy has a clear interest in high-energy particle accelerators, both for Defense Programs missions such as the production of special materials and for basic physics research. For some large accelerator projects there is currently no domestic source of ferrite rings of the needed dimensions. Gelcasting will allow a US manufacturer to compete for this business without having to make a large capital investment. The impact on the economy and on national security is clearly positive.

At the same time, the gelcasting process under development at ORNL since 1985 has until now been used only for structural ceramics. This project gave us valuable experience applying the technique to electronic materials, thereby opening up other applications of interest to Defense Programs and for high value-added components.

The CRADA activities were divided into three tasks: development and optimization of the gelcasting of soft ferrite powders, testing and evaluation of gelcast plates, and production of complex-shaped and large-toroidal soft ferrite components. The report will be presented following the task outline.

TASK I: DEVELOPMENT AND OPTIMIZATION OF THE GELCASTING OF SOFT FERRITE POWDERS

The process of developing and optimizing the gelcasting of the nickel zinc ferrite required several iterations. Three iterations were executed before sinterable gelcast ferrites were produced successfully.

First Iteration

Procedure: The partner sent the nickel zinc ferrite powder used in the CRADA. The as-received powder, CN20, dispersed poorly in the standard gelcasting premix solution, 15 wt % of monomers in water. This was attributed to the binders included in the powder in order to facilitate dry pressing. Therefore, the powders were subjected to additional treatments. The partners prepared two additional powders; XCN20-1, where their usual binders were replaced with 1/4 wt % Darvan C based on the mass of the powder, and XCN20-2, which was milled in water only without any binders. MMES prepared the powder, CN20-D, by heating the as-received powder to 800°C in air. Thus, four powders were available for the initial gelcasting tests.

The particle size and surface area of these powders were measured using a Horiba Laser Scattering Particle Size Distribution Analyzer LA-700 and a Quantachrome BET surface instrument, respectively. The results are shown in Table 1 and in Figure 1. X-ray diffraction crystallography was performed on both the as-received powder, CN20, and on the heat-treated powder, CN20-D, to determine if their crystal structures were altered during the heat treatment. The X-ray analyses are shown in Figure 2.

For each powder, 300 g plus 0.53 ml of Darvan 821-A were dispersed by milling in an attritor mill with 81.8 g of 15 wt % solution of the two gelcasting compositions, either MAM/MBAM (6:1) or MAM/PEG (3:1). Samples that were well dispersed were initiated and gelcast as shown in Table 2. Some of parts that were cast in plastic cups flaked as the samples dried. Consequently, slips were then cast in molds made of either aluminum or Teflon, and the results are reported in Table 3.

Results: The mean particle size (2.02 μm) of the CN20, the as-received powder with binders in it, and that (1.94 μm) of the XCN20-2 (powder in water only) were nearly identical as shown in Table 1. Their particle size distributions were similar. The

mean particle size (1.63 μm) of XCN20-1, powder with 1/4 wt % Darvan 821A, was slightly less than the previous two and the particle size distribution was narrower. Heat treatment seemed to have agglomerated the powder, CN20-D, which had a larger mean particle size (3.03 μm) and a wider and slightly skewed distribution. Surface area analysis confirmed these findings. The surface area of the heat-treated powder (1.70 m^2/g) was about half of that of the other three powders.

X-ray diffraction analysis indicated that the heat treatment did not change the crystal structure of the ferrite. Figures 2A and 2B show the same peaks at the same angles indicating that the nickel-zinc-iron oxide structure is identical in both powders.

As shown in Table 2, only the heat-treated powder CN20-D formed good gelled parts. Although, the XCN20-2 prepared in water only, formed a fairly well dispersed slurry, it did not gel on initiation. The slurries from the other two powders, CN20 and XCN20-1, were too thick to flow and were, therefore, not initiated.

The initial gelation studies were carried out in plastic cups. These parts, on drying, tended to flake. The results in Table 3 show that no flaking occurred with the aluminum molds. Thus, molds made out of aluminum or other metals should be used in the gelcasting of the soft ferrites. The dried non-flaking parts were sent to Ceramic Magnetics for sintering and initial evaluation (see Table 4).

Discussions & Conclusions: The powder, CN20-D, which was heat-treated to 800°C to remove all the binders before it was processed, was best suited to gelcasting. Although the calcination did cause the powder to agglomerate, X-ray analysis indicated no change in the crystal structure. Consequently, only heat-treated powders will be utilized in future iterations, provided the parts formed with these powders meet the industrial partner's specifications.

Second Iteration

Procedure: While parts gelcast from CN20-D powders treated at 800°C met the specifications (See Task II), the powders were agglomerated compared to the as-received powders. To reduce the agglomeration, the powders were treated at a lower temperature. The as-received powder was pyrolyzed in a simultaneous DTA-TGA unit (TA Instruments) to determine the amount of organic materials present and the temperature at which they were burned off. Figure 3 shows the DTA- TGA results. The as-received powder contained only ~0.25 wt % organics which was all burned off at 300°C.

The as-received powder was, therefore, heat-treated at 300°C to produce the powder, CN20-C. Additional powder, CN20-D, heat-treated at 800°C was also prepared. The particle size and specific surface area of these powders were measured. Table 5 and Figure 4 compare the particle sizes for powders heat-treated at various temperatures. Powder CN20-C, was tested in gelcasting slurries and the four parts shown in Table 6 were cast with the powder. Two were rings (~150 mm OD x 125 mm ID), made using molds of PVC tubes separated with a rubber spacer, and the other

two were plates formed in our standard aluminum molds (~ 13 mm x 100 mm x 250 mm). These parts were dried and sent to the industrial partner for evaluation.

Results and Discussions Table 5 shows that the powder, CN20-C, has a mean particle size and a specific surface area that are almost equal to those of the as-received powder. The distribution is bimodal as seen in Figure 4. The gelcasting slurry using CN20-C powder was less fluid than that with CN20-D. Nevertheless, acceptable parts were made with CN20-C and sent to the industrial partner for evaluation.

Third Iteration

Procedure: In this task, because the gelcast parts shattered and cracked during firing (see TASK II), the solids loading of the gelcasting slurry was increased from 42 to 50 vol %. This increased the green density of the gelcast ferrites and thus, should reduce the sintering shrinkage and minimize cracking. In addition, the as-received powder was heat-treated at 500°C (CN20-B), between the initial 800°C and the 300°C used in the second iteration. This was done to produce powder with decreased particle agglomeration compared to that heat-treated at 800°C which should have reduced the viscosity of the slurry compared to that of the powder treated at 300°C. The mean particle size, the size distribution, and the specific surface area of the CN20-B, heat-treated at 500°C, were measured and are included in Fig. 4 and Table 5.

Several parts formed at 50 vol % solids loading are shown in Table 7. These parts were dried by the standard procedure. Some were fired at ORNL using the modified sintering schedule, while the rest were sent to the industrial partner to densify.

Results and Discussions: Table 7 shows that only powders heat-treated at either 800 or 500°C were used in forming test parts. This was because the viscosity of the slurries with powders heat-treated at 300°C became too high as the solids loading was increased toward 50 vol %. Table 5 and Figure 4 show that powder CN20-B (500°C) has mean particle size and specific surface area that lie between those of the powders heat-treated at 300 and 800°C, respectively. However, its bimodality is more defined than that of the CN20-C (300°C) powder.

The parts sintered at MMES did not crack and had a sintered density ~98% of the theoretical value. Some of these parts were sent to the partner.

TASK II: TESTING AND EVALUATION OF GELCAST PLATES (PARTS)

There were two iterations in this task in which the industrial partner sintered and evaluated gelcast parts.

First Iteration

Procedure: Fourteen samples, which were primarily pucks and are listed in Table 4 were sent to the industrial partner. The parts were sintered by the industrial partners following the standard combined binder burn-out and sintering schedule used

for their pressed parts. The sintered parts were evaluated by measuring their magnetic and physical properties with the results shown in Table 8.

Results: Some of the parts cracked excessively during the firing cycle and as shown in Table 8 could not be evaluated. Also, because of cracking, the effect of the gelcasting premix, MAM/MBAM vs. MAM/PEG, of the accelerator ratios, and of the mold materials could not be evaluated. The heat-treated powder, CN20-D, which gelcast best, also gave satisfactory magnetic and physical properties. The initial permeabilities, μ_i , were all acceptable by the partner's specification, 800 +/- 25%. The Q measurements were high enough to yield satisfactory, high $\mu_i \times Q$ values. The bulk densities were slightly low, but firing cycle modifications may increase them.

Figures 5A and 5B show the microstructure of CN20 gelcast ferrite samples. The average grain size distributions, shown in Figure 5 A, were very good for the CN20-D castings. The XCN20-1 castings (microstructure shown in Figure 5B) were not acceptable because they either showed a wide size distribution or were bimodal.

Discussions: The result from the first samples fired and evaluated by the industrial partners show the following:

1. The parts cracked excessively during the firing cycle.
2. Only the powders that were heat-treated, CN20-D, produced parts with acceptable magnetic and physical properties.
3. Although the bulk density was low, it could be increased by sintering schedule modifications.

The firing process should be studied in order to minimize the cracking of the gelcast parts. Furthermore, only heat-treated powders will be used in all future investigations of the gelcasting of soft ferrites.

Second Iteration

Procedure & Results: The four large parts [two rings (~150 mm OD x 125 mm ID), made using molds of PVC tubes with rubber spacers and two plates cast in our standard aluminum molds (~13 mm x 100 mm x 250 mm) (Table 6)] formed with CN20-C powder (300°C) were sent to the industrial partner. The partner fired the parts using their standard firing cycle. All of the four parts shattered during the firing. Consequently, the parts were not evaluated for their magnetic and physical properties.

Discussions: Because gelcast parts were not successfully fired by the partner, MMES investigated their firing schedule, and modified it slightly based on the pyrolysis of the CN20 powder shown in Figure 3. Using the modified schedule, MMES fired parts, but these too cracked very badly. The other probable cause of the sintering cracks was attributed to excessive shrinkage. This led to the third iteration in Task I in which the solids loading of the slurry was increased from 42 to 50 vol %. Parts made in the third iteration have been sintered successfully at MMES as discussed in Task III below.

TASK III: PRODUCTION OF SOFT FERRITE PARTS (COMPLEX SHAPES AND LARGE TOROIDS)

In this task, the knowledge acquired in the other tasks was to be applied to making small parts. If these parts satisfactorily met the partner's requirements, the partner would provide molds to produce complex shapes and large toroids to be produced at MMES.

Parts were made at MMES as indicated in Table 7, some of which were fairly large. Some of these parts, five sintered and six green, were sent to the partner. Three fired parts: a large ring, a puck, and an "ORNL GELCAST" logo disc, are shown in Figure 6. However, because of the unexpected sintering problems, these parts were produced just as the CRADA was terminating. Consequently, the partner had no time to provide the molds for complex shapes and large toroids. Nevertheless, the partner was quite pleased with the parts that MMES produced. Because no domestic companies currently can produce these large, soft-magnet toroids used in high energy physics, the partner has indicated that it would pursue follow-up activities with us to make these parts.

INVENTIONS: No inventions were made or reported under this CRADA. However, the work demonstrated new applications for our existing patents (US Patents 4,894,194, 5,028,362, and 5,145,908).

CONCLUSIONS

1. Nickel zinc ferrite powders provided by the partner have been successfully formed into soft ferrite magnetic parts by the ORNL gelcasting process.
2. The gelcast parts had magnetic and physical properties that meet the partner's specifications.
3. It took several modifications of the powder and the processing steps to achieve this:
 - a. The powder was heat-treated at three different temperatures: 800, 300, and 500°C.
 - b. The solids loading of the powder in the gelcasting slurry was increased to at least 50 vol % before the parts survived sintering. Only powders heat-treated at 500 and 800°C produced fluid slurry at this solid loading and were used in gelcasting the successful parts.
 - c. The partner's standard firing schedule was modified slightly to minimize the tendency for the parts to crack during sintering.
4. Parts, as large as 125 mm OD x 100 mm ID x 25 mm rings, were fabricated and sintered to ~98% of the theoretical density. Both green and fired parts were sent to the partner.
5. The CRADA expired before the partner could provide molds to gelcast more complex shapes and large toroids. Nevertheless, the partner was pleased with the final parts delivered to it and has shown strong interest in negotiating follow-up activities to make these other shapes.

ACKNOWLEDGEMENTS

Research sponsored by the U.S. Department of Energy, Assistant Secretary for Defense Programs, Technology Management Group, Technology Transfer Initiative under contract DEAC05-84OR21400 with Lockheed Martin Energy Systems, Inc. The authors are grateful to P. Angelini, R. J. Lauf, S. D. Nunn and T. N. Tiegs for reviewing the manuscript and to C. A. Walls and D. L. Barker for assistance with the experiments.

DISCLAIMER

This report was prepared as an account of work sponsored by an agency of the United States Government. Neither the United States Government nor any agency thereof, nor any of their employees, makes any warranty, express or implied, or assumes any legal liability or responsibility for the accuracy, completeness, or usefulness of any information, apparatus, product, or process disclosed, or represents that its use would not infringe privately owned rights. Reference herein to any specific commercial product, process, or service by trade name, trademark, manufacturer, or otherwise does not necessarily constitute or imply its endorsement, recommendation, or favoring by the United States Government or any agency thereof. The views and opinions of authors expressed herein do not necessarily state or reflect those of the United States Government or any agency thereof.

List of Tables

- Table 1: The mean particle size and the surface area of the ferrite powders
- Table 2: Dispersed Samples that were Gelcast
- Table 3: Effect of Mold Material on Gelcast Parts with CN20-D Powders
- Table 4: Parts Gelcast from CN20-D (800) and XCN20-1 Powders
- Table 5: Particle Size and Surface Area of Heat-treated Ferrites
- Table 6: Parts Gelcast from CN20-C (heat-treated at 300°C) Powder
- Table 7: Parts Formed at 50 vol % Solids Loading
- Table 8: Magnetic and Physical Properties of CN20 Gelcast Ferrite Samples

List of Figures

- Figure 1: Particle Size Distribution of Ferrite Powders
- Figure 2: X-ray diffraction analysis of as-received CN20 and heat-treated CN20-D Ferrite Powders
- Figure 3: The Pyrolysis of as-received CN20 Ferrite Powder in a DTA/TGA unit.
- Figure 4: Particle Size Distribution of Additional CN20 Ferrite Powders
- Figure 5: Microstructure Of CN20 Gelcast Ferrite Samples
- Figure 6: Gelcast Soft Ferrite Parts

Table 1: The mean particle size and the surface area of the ferrite powders

<u>Powder</u>	<u>Mean Particle Size (μm)</u>	<u>Surface Area (m^2/g)</u>
CN20 (as-received)	2.02	3.65
CN20-D (800°C)	3.03	1.70
XCN20-1	1.63	3.77
XCN20-2	1.94	3.23

Table 2: Dispersed Samples that were Gelcast

Sample size: 100 g of Slurry.

<u>Sample #</u>	<u>Initiator (μl)/Catalyst (μl)</u>	<u>Result</u>
<u>A.</u>	<u>Powder: CN20-D (heat-treated) Solution: MAM/MBAM (6:1)</u>	
1	100/10	Gelled with some syneresis
2	200/20	Good gel
3	300/30	Good gel
<u>B.</u>	<u>Powder: CN20-D (heat-treated) Solution: MAM/PEG (3:1)</u>	
4	100/10	Gelled with some syneresis
5	200/20	Good gel
6	300/30	Good gel
<u>A.</u>	<u>Powder: XCN20-2 (water only) Solution: MAM/MBAM (6:1)</u>	
7	100/10	No gelation
8	200/20	No gelation
9	300/30	No gelation

Table 3: Effect of Mold Material on Gelcast Parts with CN20-D Powders

<u>Sample #</u>	<u>Initiator ($\mu\text{l/g}$)/Catalyst ($\mu\text{l/g}$)</u>	<u>Mold</u>	<u>Gelation</u>	<u>Drying Result</u>
<u>A. Solution: MAM/MBAM (6:1)</u>				
1	0.2/0.02	Aluminum	Gel	Good
2	0.2/0.02	Aluminum	Gel	Good
3	0.2/0.02	Teflon	Gel	Flaking
<u>B. Solution: MAM/PEG (3:1)</u>				
4	0.2/0.02	Aluminum	Gel	Good
5	0.2/0.02	Aluminum	Gel	Good
6	0.2/0.02	Teflon	Gel	Flaking

Table 4: Parts Gelcast from CN20-D (800) and XCN20-1 Powders

<u>Sample</u>	<u>System</u>	<u>Mold Material</u>	<u>TEMED/APS/g Slip</u>
1 - XCN20-1	MAM/PEG 3:1	Polyethylene	0.01 μl / 0.1 μl
2 - XCN20-1	MAM/PEG 3:1	Polyethylene	0.02 μl / 0.2 μl
3 - CN20-D	MAM/MBAM 6:1	Polyethylene	0.03 μl / 0.3 μl
4 - CN20-D	MAM/MBAM 6:1	Polyethylene	0.02 μl / 0.2 μl
5 - CN20-D	MAM/MBAM 6:1	Polyethylene	0.01 μl / 0.1 μl
6 - CN20-D	MAM/PEG 3:1	Polyethylene	0.02 μl / 0.2 μl
7 - CN20-D	MAM/PEG 3:1	Polyethylene	0.03 μl / 0.3 μl
8 - CN20-D	MAM/PEG 3:1	Polyethylene	0.01 μl / 0.1 μl
9 - CN20-D	MAM/MBAM 6:1	Aluminum	0.02 μl / 0.2 μl
10 - CN20-D	MAM/MBAM 6:1	Aluminum	0.02 μl / 0.2 μl
11 - CN20-D	MAM/MBAM 6:1	Teflon	0.02 μl / 0.2 μl
12 - CN20-D	MAM/PEG 3:1	Aluminum	0.02 μl / 0.2 μl
13 - CN20-D	MAM/PEG 3:1	Aluminum	0.02 μl / 0.2 μl
14 - CN20-D	MAM/PEG 3:1	Teflon	0.02 μl / 0.2 μl

Table 5: Particle Size and Surface Area of Heat-treated Ferrites

<u>CN20 Powder</u>	<u>Mean Particle Size (μm)</u>	<u>Specific Surface Area (g/m^2)</u>
CN20 (As-received)	1.78	3.37
CN20-D (800°C)	3.37	1.43
CN20-C (300°C)	1.89	3.22
CN20-B (500°C)	2.10	2.72

Table 6: Parts Gelcast from CN20-C (heat-treated at 300°C) Powder

<u>Sample</u>	<u>System</u>	<u>Mold Material</u>	<u>TEMED/APS/g Slip</u>
15 - Ring	MAM/MBAM 6:1	PVC + Rubber	0.03 μl / 0.3 μl
16 - Ring	MAM/PEG 3:1	PVC + Rubber	0.03 μl / 0.3 μl
17 - Plate	MAM/PEG 3:1	Aluminum	0.03 μl / 0.3 μl
18 - Plate	MAM/MBAM 6:1	Aluminum	0.03 μl / 0.3 μl

Table 7: Parts Formed at 50 vol % Solids Loading

<u>Sample</u>	<u>System</u>	<u>CN20 Powder</u>
<u>A - Sintered Parts</u>		
1-Large Ring	MAM/MBAM 6:1	CN20-D (800°C)
2-ORNL logo	MAM/MBAM 6:1	CN20-D (800°C)
3-Puck	MAM/MBAM 6:1	CN20-B (500°C)
4-Puck	MAM/PEG 3:1	CN20-B (500°C)
5-Puck	MAM/MBAM 6:1	CN20-B (500°C)
<u>B - Green Parts</u>		
6-Large Ring	MAM/MBAM 6:1	CN20-B (500°C)
7-Puck	MAM/MBAM 6:1	CN20-B (500°C)
8-Puck	MAM/MBAM 6:1	CN20-B (500°C)
9-Large Ring	MAM/PEG 3:1	CN20-B (500°C)
10-Puck	MAM/PEG 3:1	CN20-B (500°C)
11-Puck	MAM/PEG 3:1	CN20-B (500°C)

Ceramic Magnetics, Inc.

16 LAW DRIVE, FAIRFIELD, N.J. 07004-2404
 (201) 227-4222 FAX (201) 227-6735

Table 8: Magnetic and Physical Properties of CN20 Gelcast Ferrite Samples

SAMPLE NUMBER	FIRE NUMBER	0.5 MHz		DENSITY, gm/cc	GRAIN Size, um	
		<u>ui</u>	<u>Q</u>			
CMI Spec.		800 +/-25%		2.8 nom	5.21 nom	14 nom
1	835-94	720	41	3.0	5.23	bimodal
2	945-94	750	44	3.3	5.11	bimodal
3	835-94	910	27	2.5	5.15	14
4	835-94	cracked, no toroids			5.16	12
5	945-94	860	30	2.6	5.18	14
6	945-94	cracked, no samples		-----		
7	945-94	880	30	2.6	5.14	14
8	945-94	cracked, no samples		-----		
9	835-94	920	27	2.5	5.13	12
10	809-94	985	32	3.2	5.05	--
11	945-94	880	29	2.6	5.13	11
12	945-94	cracked, no samples		-----		
13	burned-out only, cracks		-----			
14	835-94	920	27	2.5	5.12	12

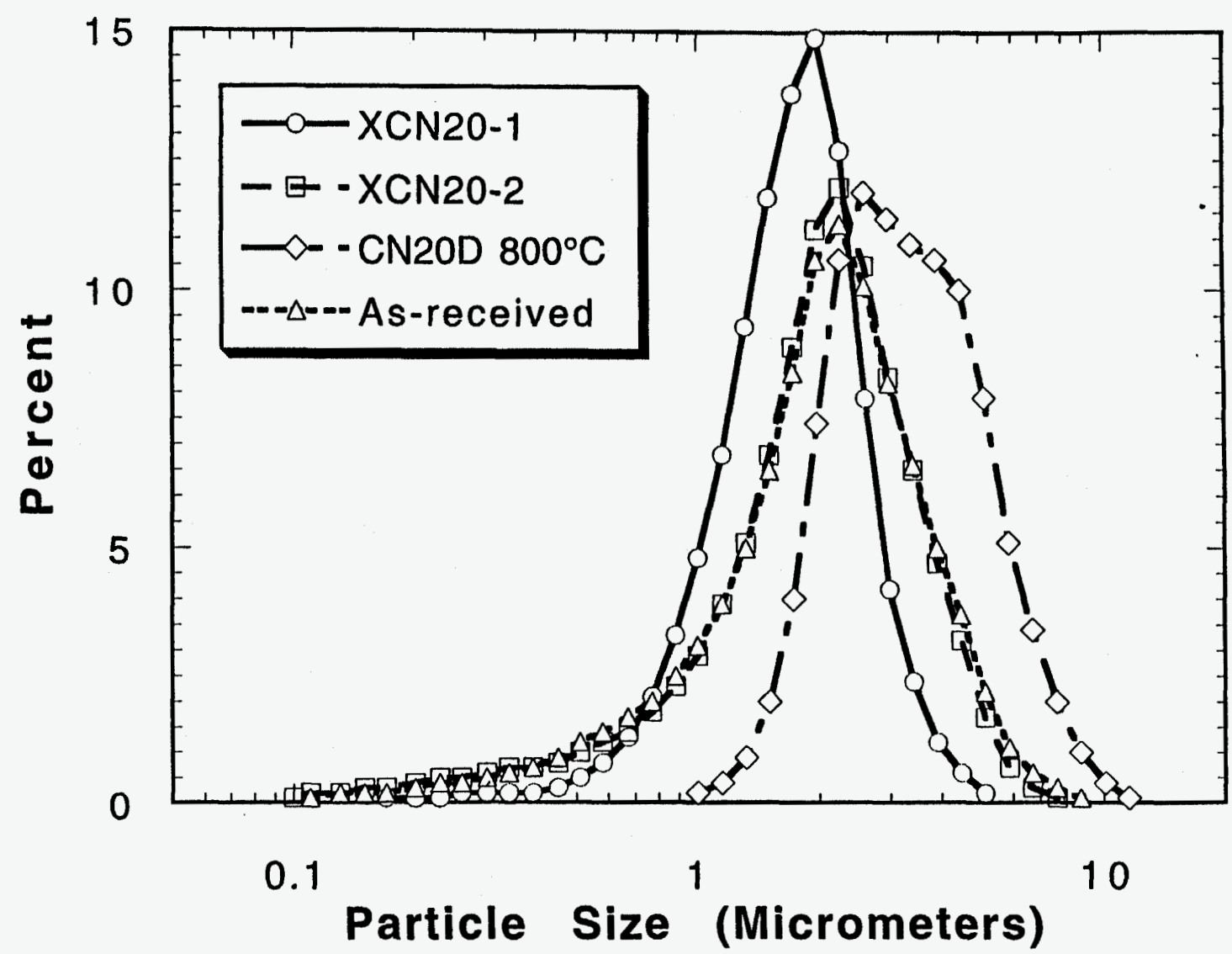


Figure 1: Particle Size Distribution of Ferrite Powders.



FN: D00405.NI
DATE: 05/31/94

ID: CN20 AS RECEIVED
TIME: 09: 51 PT: 1.20000

SCINTAG/USA
STEP: 0.02000 WL: 1.54060

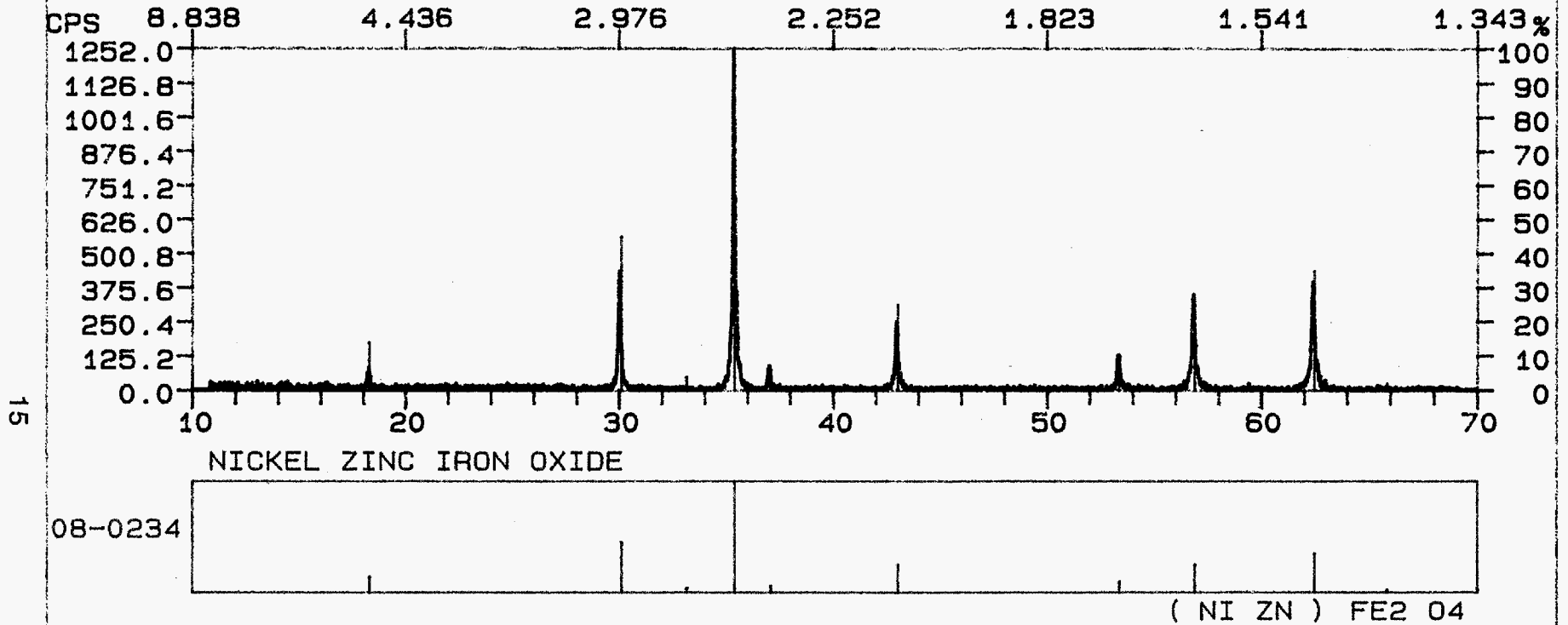
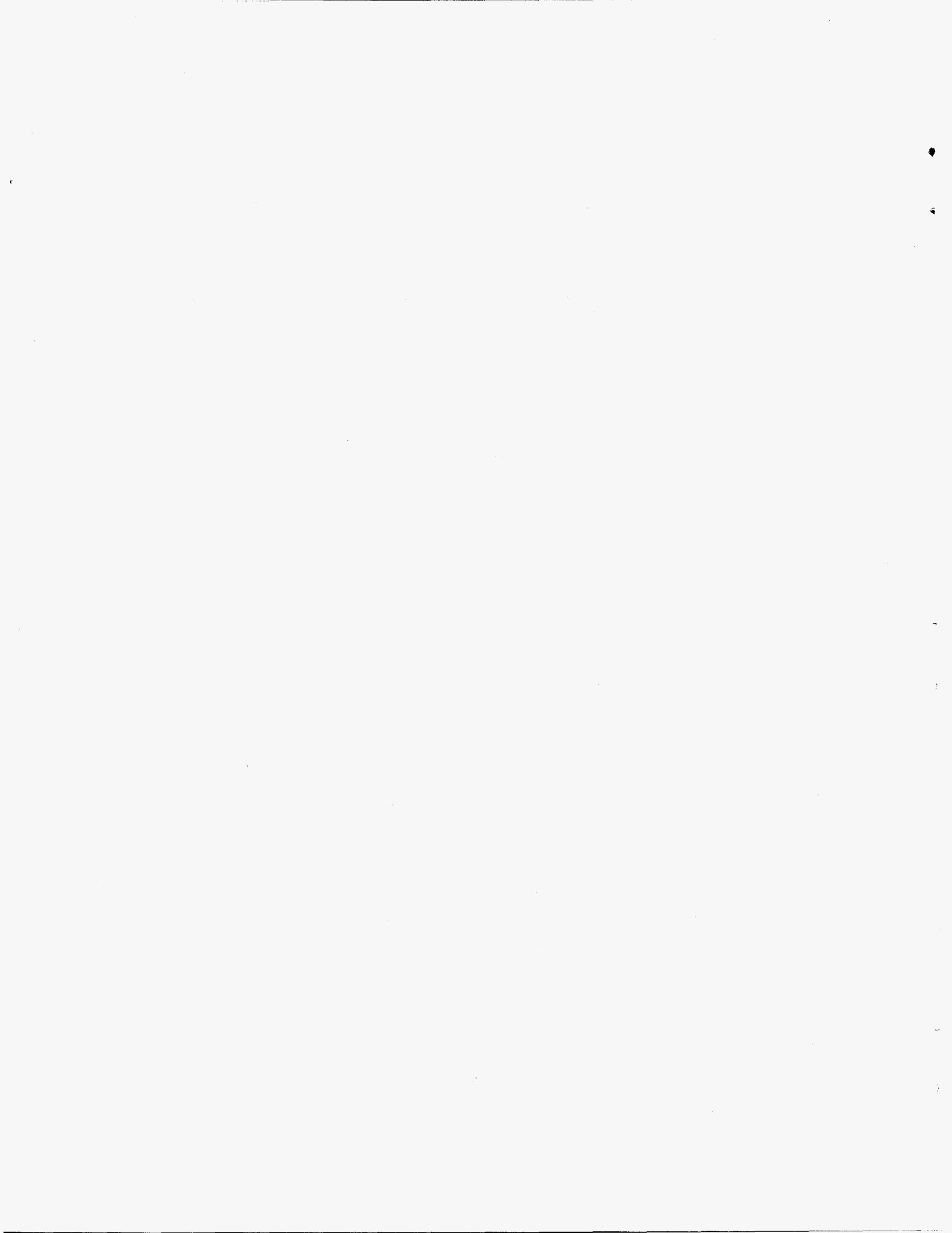
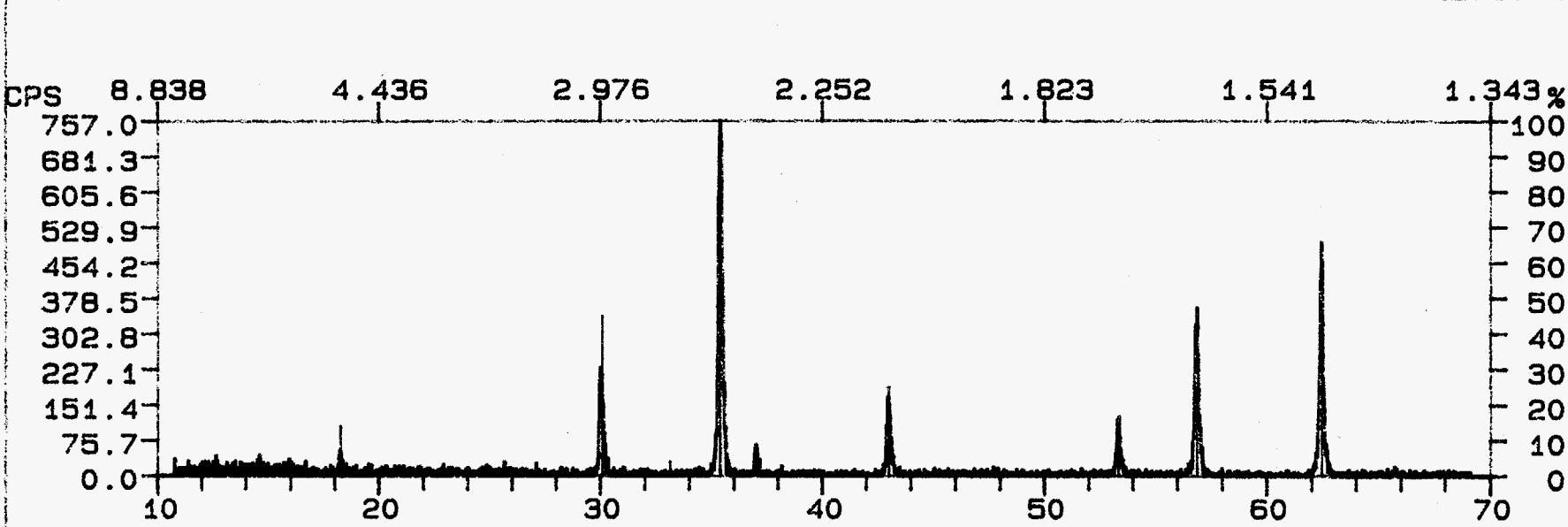


Figure 2A: X-ray diffraction analyses of CN20 as-received Powder



FN: D00406.NI ID: CN20 DEBINDERED SCINTAG/USA
 DATE: 05/31/94 TIME: 15; 21 PT: 1.20000 STEP: 0.02000 WL: 1.54060

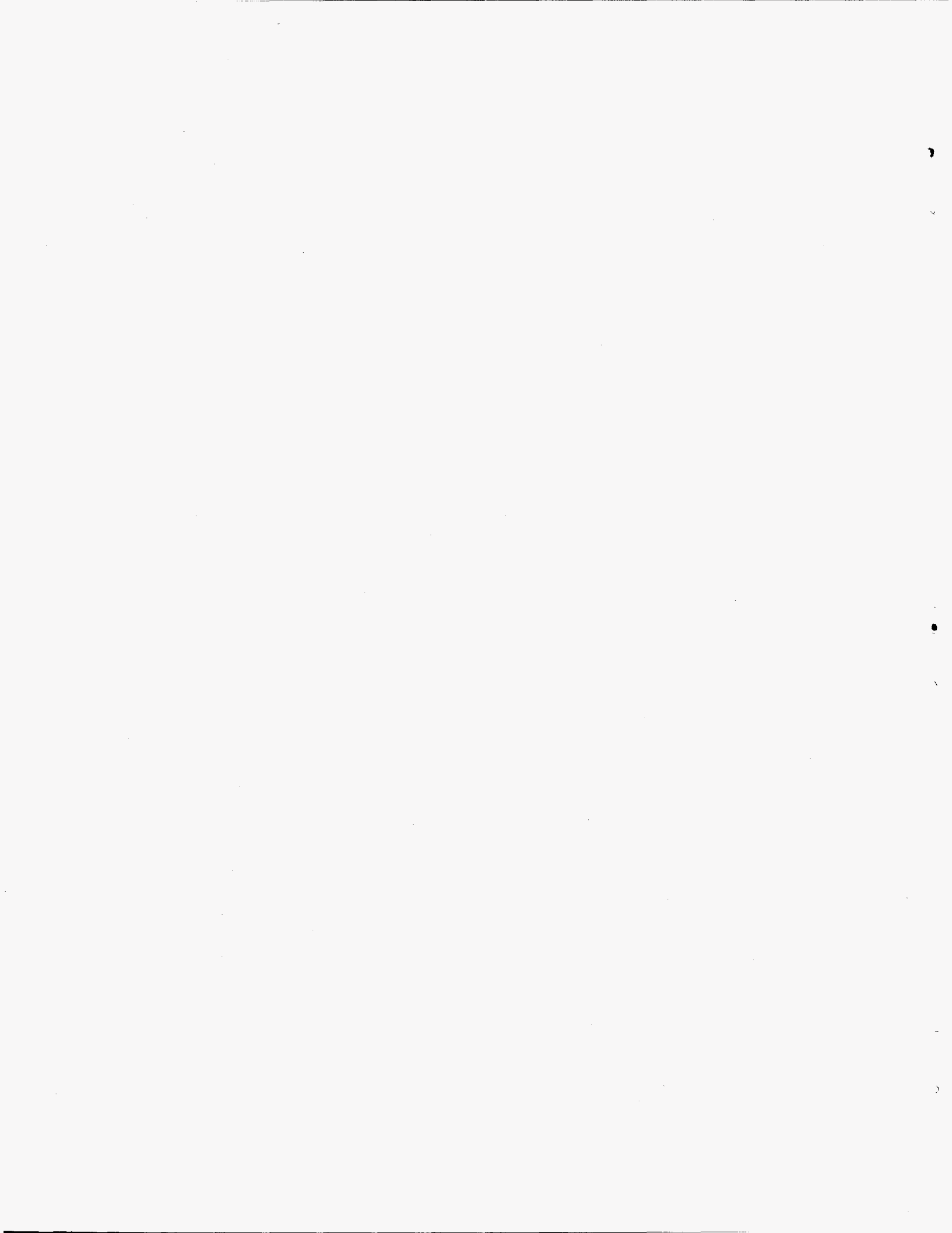


NICKEL ZINC IRON OXIDE



(NI ZN) FE2 O4

Figure 2B: X-ray diffraction analyses of CN20-B calcined at 800°C



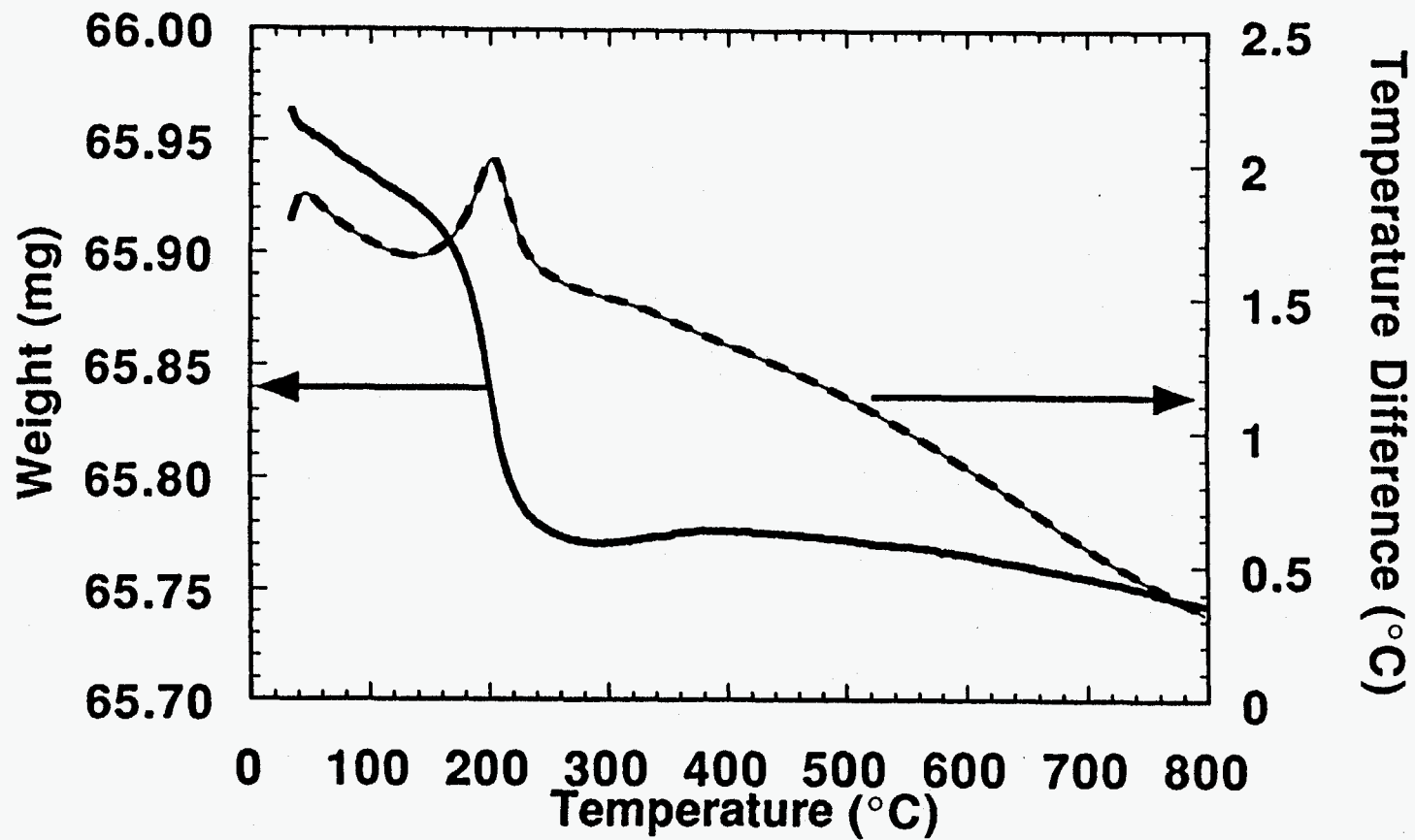


Figure 3: The Pyrolysis of as-received CN20 Powder in a DTA/TGA unit.

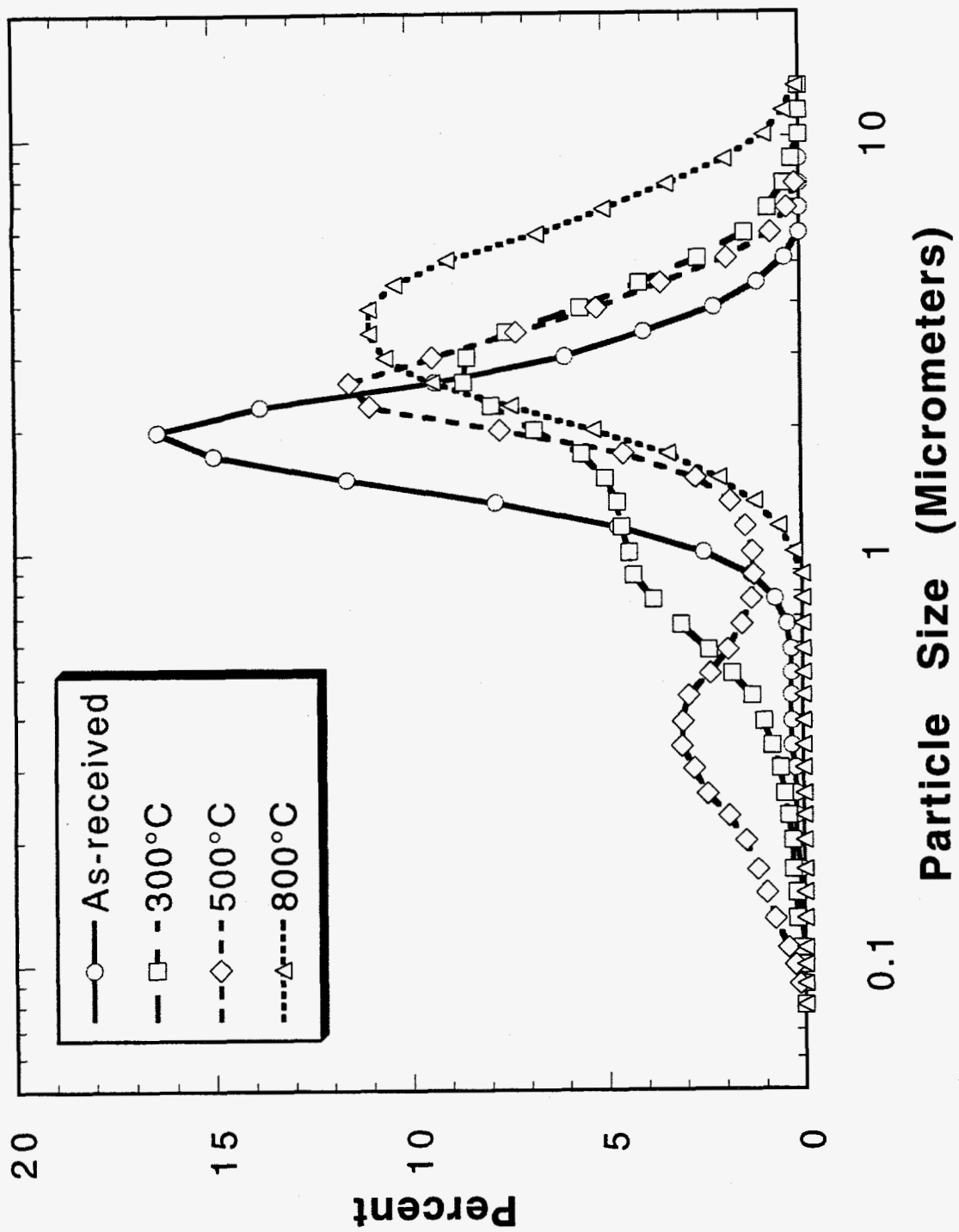


Figure 4: Particle Size Distribution of Additional CN20 Ferrite Powders.

Figure 5: Microstructure of CN20 Gelcast Ferrite Samples

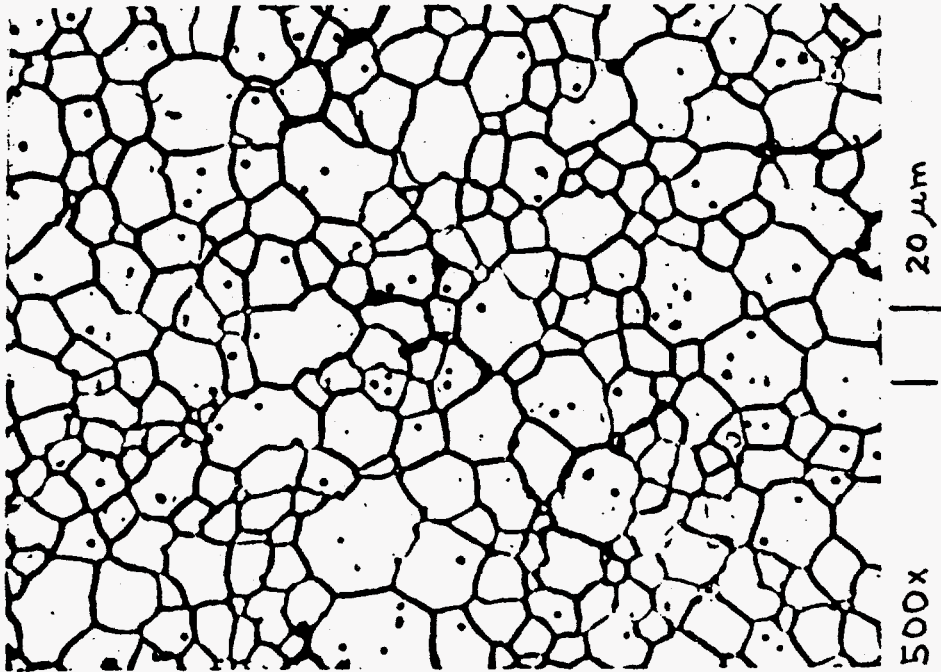


Fig. 5A: Typical CN20-D (Samples 3-14)



Fig. 5B: Typical XCN20-1 (Samples 1&2)

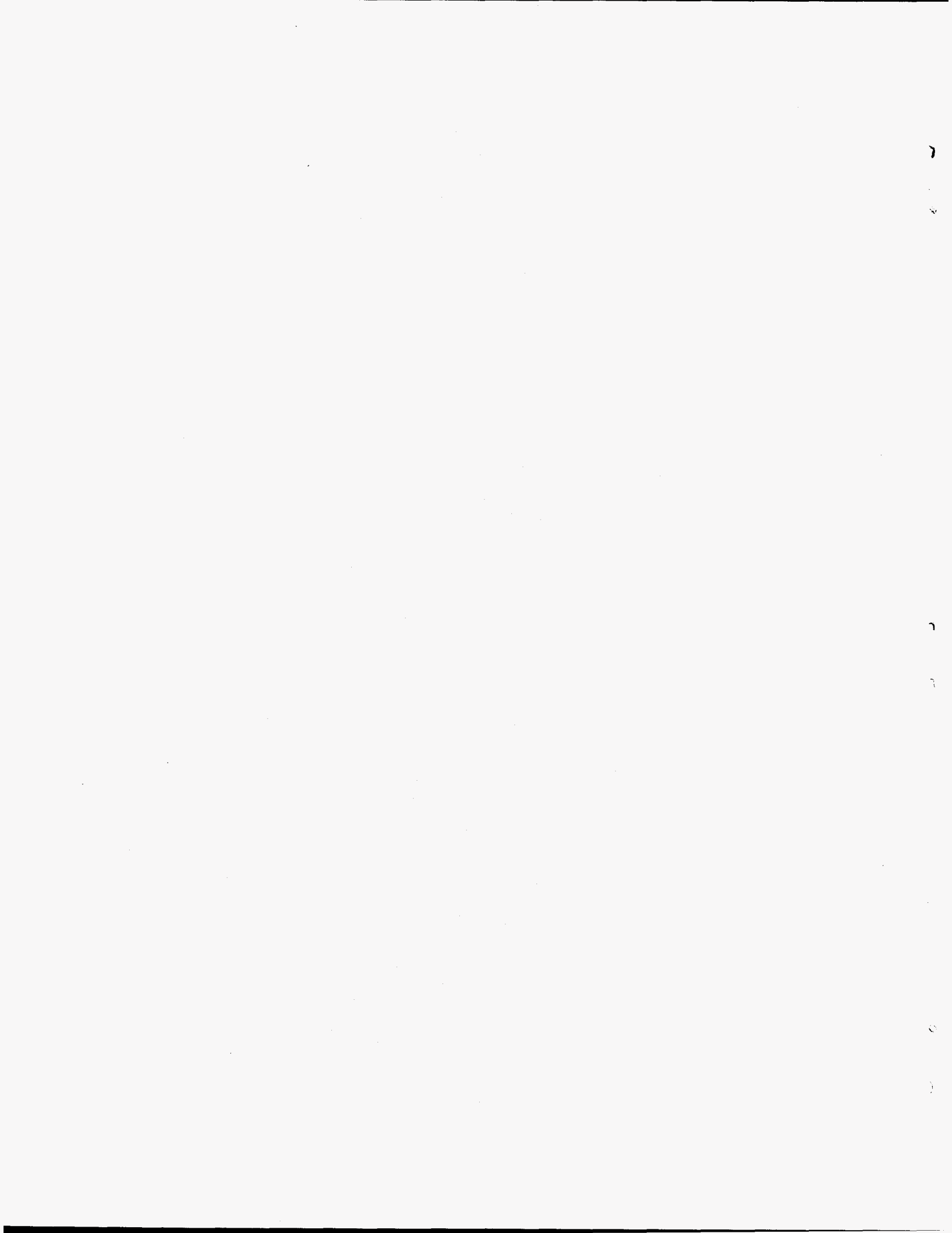
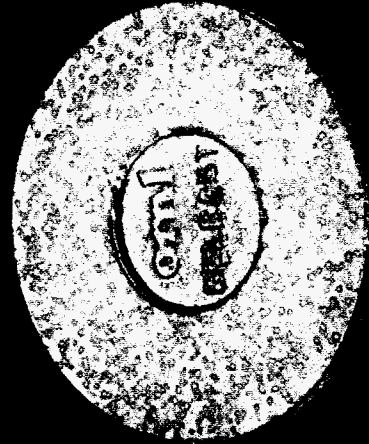
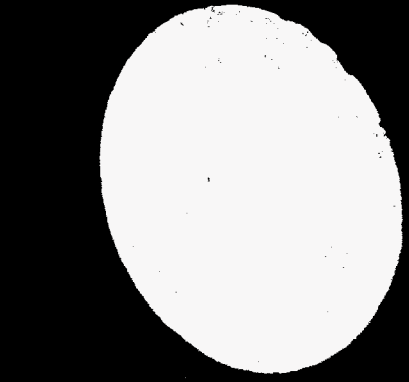
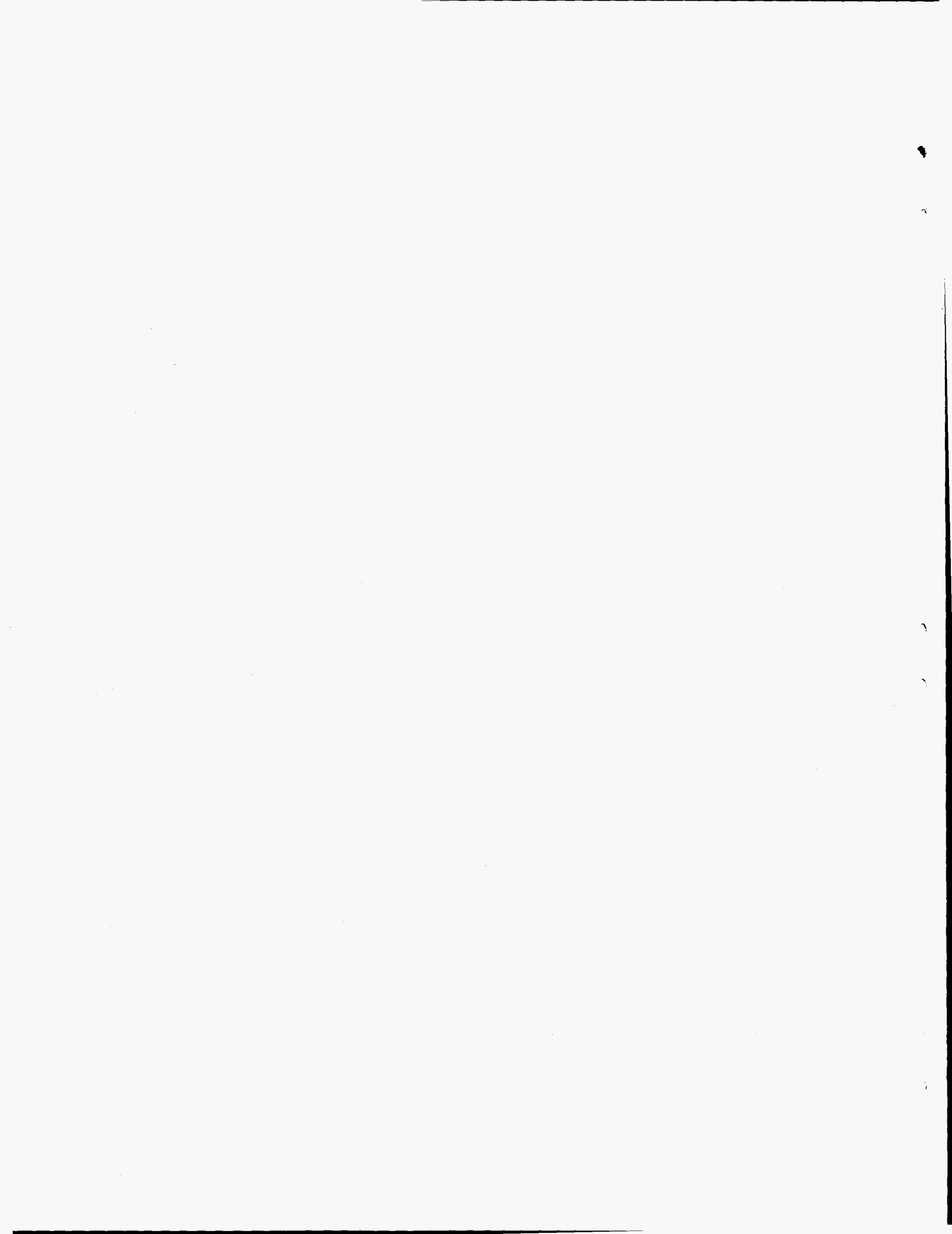


FIGURE 6: GELCAST SOFT FERRITE PARTS

CN-20 FERRITE GELCAST & SINTERED



omni



INTERNAL DISTRIBUTION

1.	P. Angelini	15.	A. J. Moorhead
2.	R. L. Beatty	16.	S. D. Nunn
3.	R. A. Bradley	17-21.	O. O. Omatete
4-5.	B. B. Bovee	22.	W. P. Painter
6.	R. H. Cooper, Jr.	23.	R. S. Steele, Jr.
7.	A. Choudhury	24.	T. N. Tieg
8.	D. F. Craig	25.	C. A. Walls
9.	L. B. Dunlap	26-27.	Central Research Library
10.	L. L. Horton	28.	Document Reference Library
11.	M. A. Janney	29-30.	Laboratory Records Department
12.	J. O. Kiggans, Jr.	31-33.	M&C Records Office
13.	H. D. Kimrey	34.	ORNL Patent Section
14.	R. J. Lauf		

EXTERNAL DISTRIBUTION

35-39. CERAMIC MAGNETICS, INC., 16 Law Drive, Fairfield, NJ 07004-3207
G. L. Van Dillen, Jr.

40-41. U.S. DOE, OFFICE OF SCIENTIFIC AND TECHNICAL INFORMATION,
P.O. Box 62, Oak Ridge, TN 37831

